Journal of Medicinal Chemistry

pubs.acs.org/jmc Article

Novel Carboline Fungal Histone Deacetylase (HDAC) Inhibitors for Combinational Treatment of Azole-Resistant Candidiasis

Zhuang Li, Jie Tu, Guiyan Han, Na Liu,* and Chunquan Sheng*

Cite This: *J. Med. Chem.* 2021, 64, 1116−1126 Read Online

ACCESS | Metrics & More | Article Recommendations | Supporting Information

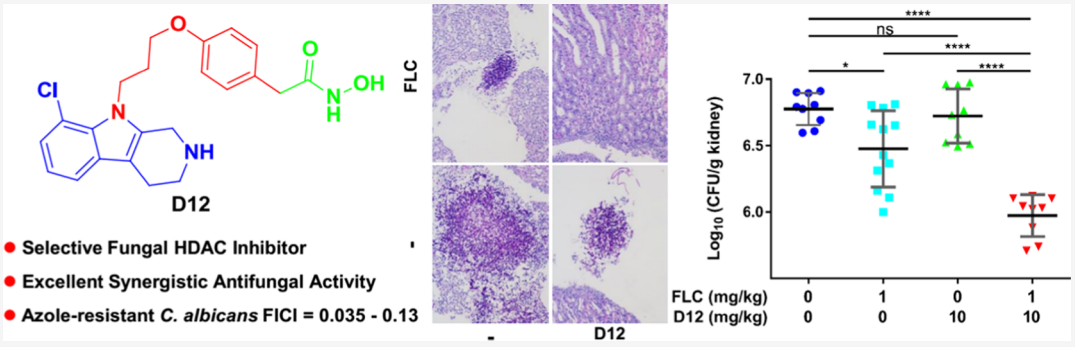

ABSTRACT: Due to the evolution and development of antifungal drug resistance, limited efficacy of existing drugs has led to high mortality in patients with serious fungal infections. To develop novel antifungal therapeutic strategies, herein a series of carboline fungal histone deacetylase (HDAC) inhibitors were designed and synthesized, which had potent synergistic effects with fluconazole against resistant *Candida albicans* infection. In particular, compound **D12** showed excellent *in vitro* and *in vivo* synergistic antifungal efficacy with fluconazole to treat azole-resistant candidiasis. It cooperated with fluconazole in reducing the virulence of *C. albicans* by blocking morphological mutual transformation and inhibiting biofilm formation. Mechanism studies revealed that the reversion of drug resistance was due to downregulation of the expression of the azole target gene *ERG11* and efflux gene *CDR1*. Taken together, fungal HDAC inhibitor **D12** offered a promising lead compound for combinational treatment of azole-resistant candidiasis.

INTRODUCTION

Invasive fungal infections (IFIs) have been increasingly realized as a lethal threat to immunocompromised and critical patients in clinic. It is estimated that the number of deaths caused by IFIs reaches 1.5 to 2 million per year.[1] About 17% intensive care unit (ICU) patients suffer from candidiasis.[2] Due to the high survival ability in the bloodstream, *Candida albicans* is the most common fungal pathogen.[1−4] Currently, only four types of antifungal drugs (azoles, polyenes, echinocandins, and flucytosine) are approved to treat fungal infections, whose therapeutic effects are limited by low potency and high toxicity.[5,6] A single type of antifungal agent could easily lead to the rapid evolution and development of drug resistance, and in most cases, higher mortality is closely associated with the drug-resistant fungal infection.[7,8] Therefore, there is an urgent need to develop novel antifungal agents or drug combinations with synergistic effects to expand current therapeutic strategies.

Combinational drug therapy is one of the promising strategies that could enhance the efficacy of first-line drugs and block the emergence of drug resistance.[9,10] Drug resistance of fungi involves transcriptional regulation, in which chromatin kinetics and histone modification play a major role.[4] Histone modification, regulated by HDACs, plays a vital role in stress-signaling responses, which is related to fungal adaptation to various environmental stresses including drug stress.[4,11] Fungal HDACs participate in fungal infection and resistance through various ways, including limiting fungal development, reducing fungal virulence, and preventing its dissemination. It is reported that the combination of HDAC inhibitors and azole drugs has synergistic antifungal effects against azole-resistant *C. albicans*.[12−15] However, human HDAC inhibitors are mostly developed as antitumor agents, which hamper their direct use as synergistic antifungal agents. Thus, there is an urgent need to develop fungal HDAC inhibitors with improved selectivity and synergistic potency and reduced cytotoxicity.

In our previous studies, we designed lanosterol 14α-demethylase (CYP51)-HDAC[16] and Janus kinase 2 (JAK2)-HDAC6[17] dual inhibitors for the treatment of resistant

Received: October 7, 2020
Published: December 27, 2020

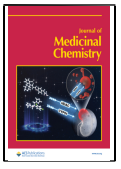

https://dx.doi.org/10.1021/acs.jmedchem.0c01763
J. Med. Chem. 2021, 64, 1116−1126

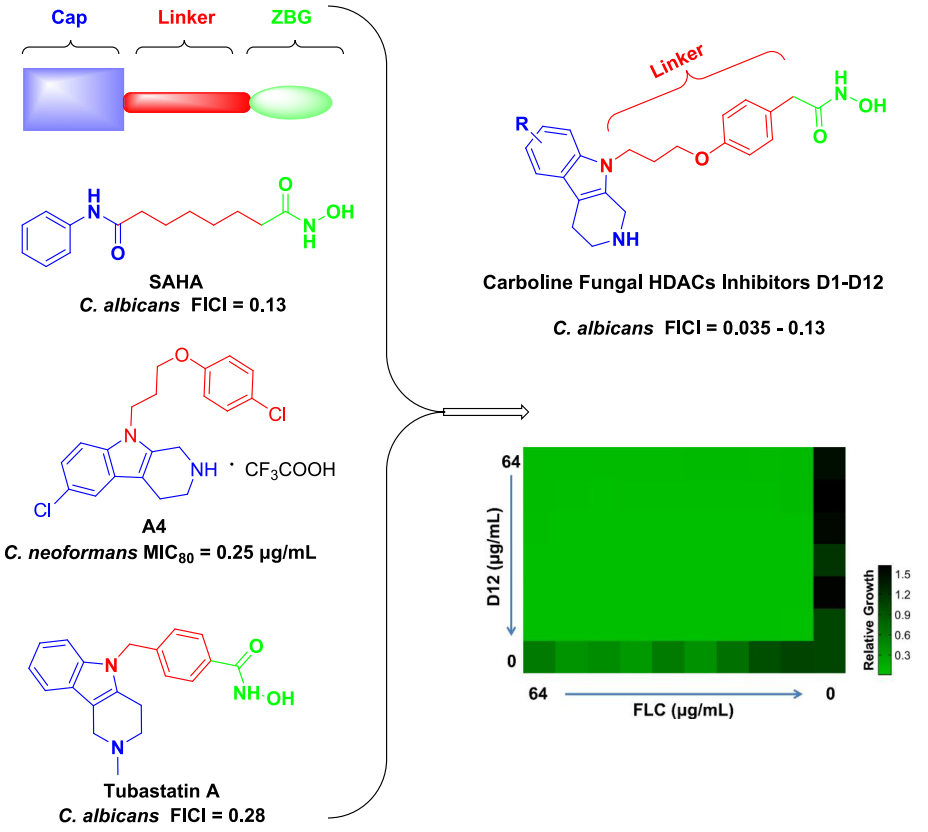

Figure 1. Design of carboline compounds as novel fungal HDAC inhibitors. The fraction inhibitory concentration index (FICI) is defined as the sum of the ratios that divide the MIC value of each drug used in combination by the value of the drug used alone. Synergism and antagonism were defined by FICIs of ≤0.5 and >4, respectively. An FICI > 0.5 but <4 is considered irrelevant. The subfigure at the bottom right is the antifungal activity in the form of a heat map measured by the checkerboard microdilution assay. The relative growth of fungi (0−1.5) changes from green to black (the greener the color, the stronger the inhibition).

Scheme 1. Chemical Synthesis of Carboline Compounds[a]

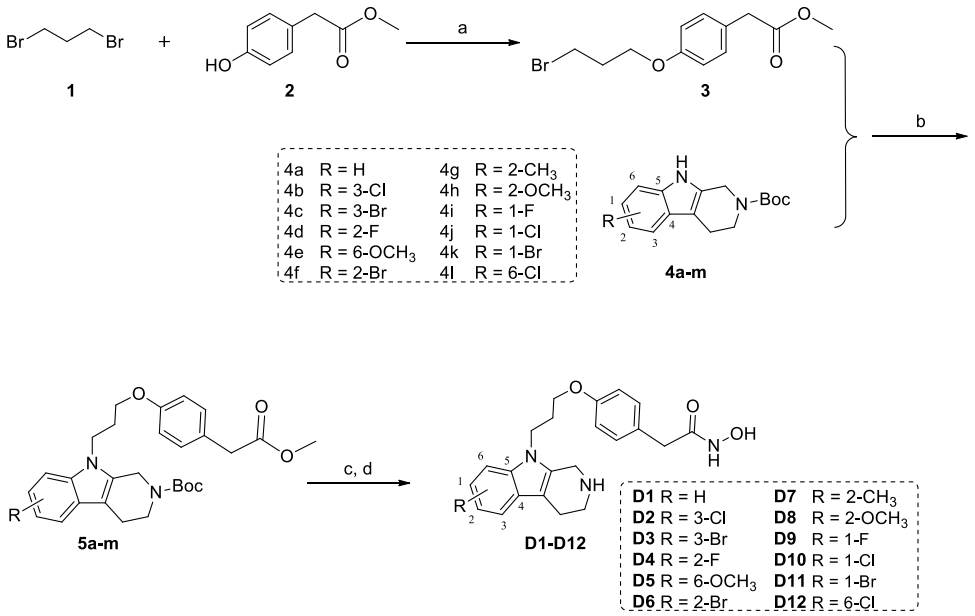

[a]**Reagents and conditions:** (a) K_2CO_3, CH_3OH, yield 64%; (b) NaH, dimethylformamide (DMF), yield 24−85%; (c) trifluoroacetic acid (TFA), CH_2Cl_2; and (d) KOH, $NH_2OH{\cdot}HCl$, and CH_3OH, yield 31−84%.

candidiasis. In particular, the HDAC6/JAK2 dual inhibitors showed excellent synergistic effects with fluconazole (FLC) to treat resistant *C. albicans* infections. Inspired by the results, we further assayed the synergistic effects of tubastatin A (TBA), a selective HDAC6 inhibitor, with azole antifungal agents. The results revealed that TBA synergized with FLC, voriconazole

https://dx.doi.org/10.1021/acs.jmedchem.0c01763
J. Med. Chem. 2021, 64, 1116−1126

(VRC), and itraconazole (ITC) against resistant *C. albicans* isolates (Table S1 in the Supporting Information). Thus, HDAC6 inhibitor TBA offered a lead compound for discovering novel synergistic antifungal agents. To further improve the antifungal activity and clarify the structure−activity relationships (SARs), herein a series of carboline compounds were designed and synthesized on the basis of our previously identified carboline antifungal scaffold[18] (Figure 1). Most compounds were able to potentiate the antifungal activity of FLC against FLC-resistant *C. albicans* cells. In particular, the combination of compound **D12** and FLC effectively blocked the morphological changes and biofilm formation of *C. albicans* and showed potent *in vivo* efficacy in a model of resistant candidiasis.

RESULTS AND DISCUSSION

Design of Carboline HDAC Inhibitors. The pharmacophores of typical HDAC inhibitors can be divided into three parts: a cap group, a linker (usually hydrophobic), and a zinc-binding group (ZBG). In particular, ZBG (hydroxamic acid or benzamide group) binds to the zinc ion and plays a crucial role in the inhibition of zinc-dependent HDACs.[19] Typically, TBA consists of a carboline cap group, a benzyl linker, and a hydroxamic acid ZBG group. On the basis of our previous work, the β-carboline ring was proven to be a potent antifungal scaffold,[18] which was selected as the cap group and the hydroxamic acid ZBG necessary for HDAC binding was retained. Considering the structural features of TBA and carboline lead compounds, the propoxy phenyl group was designed as the linker and various substitutions were introduced on the carboline scaffold (**D1−12**, Figure 1).

Chemistry. The chemical synthesis of carboline compounds is described in Scheme 1. Intermediates **4a−m** were synthesized according to our previous methods by using various substituted indoles as starting materials.[18] A substitution reaction between intermediate **3** and intermediates **4a−m** was performed in the presence of NaH to give products **5a−m**. Target compounds (**D1−12**) were obtained via two steps including the removal of the *t*-butoxycarbonyl protective group in intermediates **5a−m** and the nucleophilic addition reaction with hydroxylamine.

Carboline Derivatives in Combination with FLC Inhibited Azole-Resistant *C. albicans*. The antifungal activities of TBA and carboline derivatives used alone or in combination with FLC are listed in Table 1. The minimum concentration of 80% inhibition (MIC_{80}) is defined as the lowest concentration of a drug alone or synergistically that inhibits fungal cell growth by 80%. Carboline derivatives generally were inactive in inhibiting the growth of FLC-resistant *C. albicans* ($MIC_{80} \geq 64$ μg/mL) when used alone. In contrast, they showed synergistic effects with FLC and the antifungal activities of compounds **D1−12** in combination with FLC were significantly enhanced. The MIC_{80} values were reduced from >64 μg/mL to 0.25−8 μg/mL with the FICI values ranging from 0.035 to 0.13. Compounds **D1−12** were also tested for the synergistic effects with other azoles (VRC and ITC) against azole-resistant *C. albicans*, which also showed excellent synergistic activities (FICI = 0.035−0.13, Table S2 in the Supporting Information). Thus, carboline compounds could enhance the efficacy of azole drugs against azole-resistant *C. albicans* and reverse the development of antifungal drug resistance. Among them, compound **D12** showed the best synergistic effect and could be considered as a potential lead compound for the combinational treatment of candidiasis.

Table 1. *In Vitro* Antifungal Activity of Compounds Used Alone or in Combination with FLC against the *C. albicans* Strain (0304103) by the Checkerboard Microdilution Assay

	compounds		FLC		
	alone	synergetic	alone	synergetic	FICI[a]
D1	>64	4	>64	0.5	0.070
D2	>64	2	>64	0.5	0.039
D3	>64	4	>64	0.25	0.066
D4	>64	2	>64	2	0.062
D5	>64	2	>64	1	0.047
D6	64	2	>64	0.25	0.035
D7	>64	4	>64	1	0.078
D8	>64	8	>64	0.5	0.13
D9	>64	2	>64	1	0.047
D10	64	2	>64	1	0.047
D11	>64	2	>64	0.5	0.039
D12	>64	2	>64	0.25	0.035
SAHA	>64	8	>64	025	0.13
TBA	>64	16	>64	2	0.28

[a]Synergism and antagonism were defined by FICIs of ≤0.5 and >4, respectively. An FICI > 0.5 but < 4 is considered irrelevant.

Inspired by the synergistic antifungal effect of compound **D12** and FLC, a series of clinically isolated strains were selected to further verify whether **D12** also has a broad synergic activity against various types of *Candida* spp. As shown in Table 2, compound **D12** showed excellent synergistic antifungal activity against all of these strains when used in combination with FLC (FICI range: 0.035−0.25). Compared with TBA, compound **D12** had a better synergistic effect against all of the tested strains. It is worth noting that TBA had no synergistic effect on *Candida krusei*, while compound **D12** had an FICI of 0.25 (Table 2 and Figure S1 in the Supporting Information). The synergistic activities of compound **D12** in combination with VRC and ITC against other clinical strains such as *Candida auris*, *Candida glabrata* (*Cornus glabrata*), *Candida tropicalis*, and *Cryptococcus neoformans* were further tested. The results revealed that compound **D12** had synergistic effects with azoles against most *Candida* species, whereas the synergism was lost against *C. neoformans* (Table S3 in the Supporting Information). Therefore, compound **D12** represents a lead compound for potential antifungal combination therapy, whose *in vitro* and *in vivo* antifungal activities and antiresistance mechanisms were further investigated.

Compound D12 Blocked the Emergence of Fungal Resistance Combined with FLC and the Synergism Mainly Depended on Compound D12 Rather than FLC. To validate the synergistic effect of compound **D12** more intuitively, its ability to block the emergence of azole resistance was tested. It was observed that drug resistance appeared in a high concentration of FLC (32 μg/mL) or a medium concentration of compound **D12** (8 μg/mL). But no colony occurred on the medium containing both FLC and compound **D12** at the same concentration (Figure 2A). In Figure 2B, it could be observed that compound **D12** could enhance the antifungal effects of FLC in a dose-dependent manner by comparing the size of the inhibition ring. Thus, the combination of compound **D12** and FLC blocked the emergence of FLC resistance and enhanced the efficacy of FLC. However, it still remains unclear what the relationship

https://dx.doi.org/10.1021/acs.jmedchem.0c01763
J. Med. Chem. 2021, 64, 1116−1126

Table 2. *In Vitro* Synergistic Effect of Compound D12 When Used in Combination with FLC against Various *C. albicans* Strains and *C. krusei* Strains

	MIC_{80} (μg/mL)									
	alone		synergetic			alone		synergetic		
strains[a]	D12	FLC	D12	FLC	FICI	TBA	FLC	TBA	FLC	FICI
9172	>64	>64	2	0.5	0.039	>64	>64	16	0.5	0.26
9884	64	>64	2	0.5	0.039	>64	>64	4	1	0.078
10061	>64	>64	2	2	0.062	>64	>64	2	0.5	0.039
4108	64	>64	2	0.25	0.035	>64	>64	8	0.5	0.13
10153	64	64	8	8	0.25	>64	64	64	32	1.5

[a]*C. albicans* strains include 9172, 9884, 10061, and 4108. The *C. krusei* strain includes 10153.

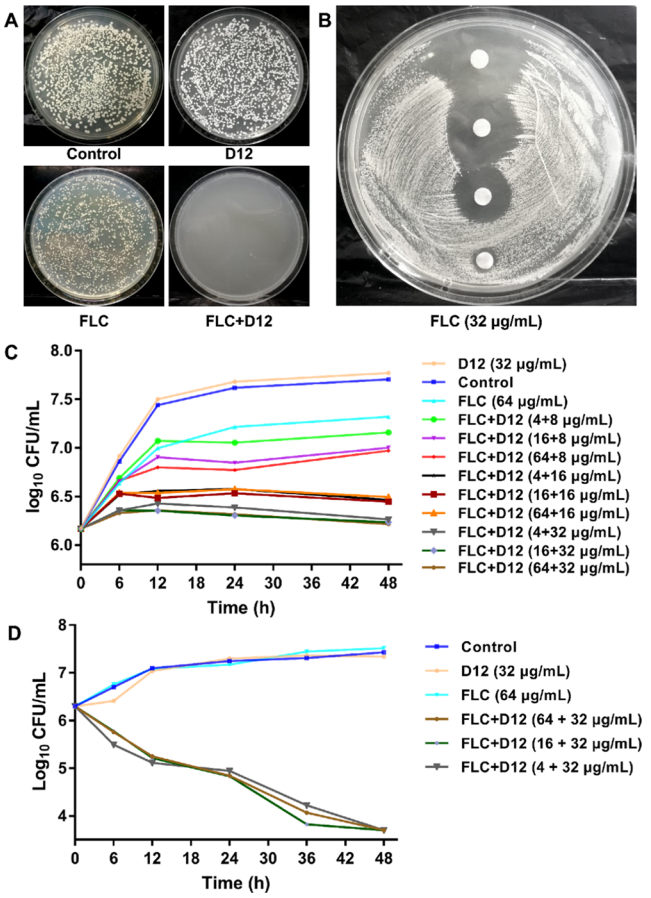

Figure 2. Compound **D12** cooperates with FLC to block the emergence of drug resistance and plays a major role in the synergistic process. (A) Compound **D12** blocks the emergence of FLC resistance in *C. albicans* (0304103). In total, 1×10^4 cells were plated on the Sabouraud Dextrose Agar (SDA) medium containing no drugs (Control), compound **D12** (8 μg/mL), FLC (32 μg/mL), or the combination. Plates were photographed 48 h after incubation at 35 °C. (B) FLC and compound **D12** are synergistic against *C. albicans*. Disks containing compound **D12** were plated on the plate containing FLC (32 μg/mL). The doses of compound **D12** on the disks were 32, 8, 2, and 0 μg from the top to the bottom. Experiments could be duplicated biologically. (C) Time growth curves of the *C. albicans* strain 0304103 under different concentrations of compounds. The initial concentration of *C. albicans* was 1.5×10^6 cells/mL. The number of cells was counted at a specific time point (0, 6, 12, 24, 48 h) and the concentration was calculated. (D) Time kill curves of *the C. albicans* strain 0304103 when compound **D12** (32 μg/mL) was used in combination with different concentrations of FLC. Three independent experiments were performed.

between FLC and compound **D12** is, and which is more important in suppressing the emergence of fungal resistance. Therefore, the relationship between the synergism and the concentration of the two drugs was investigated. Single use of compound **D12** (32 μg/mL) or FLC (64 μg/mL) led to no or weak antifungal activity. In contrast, the growth of fungi was inhibited markedly when the two drugs were used in combination (Figure 2C). In addition, after fixing FLC to a specific concentration (4, 16, or 64 μg/mL), the inhibitory effect was dependent on the concentration of compound **D12**. In contrast, changing the concentration of FLC with a specific value of compound **D12** (8, 16, or 32 μg/mL) had no significant impact on the antifungal activity. These results indicated that compound **D12** not only enhanced the activity of FLC, but also played a major role in the synergistic effects. For further investigating the synergistic antifungal mechanism, the fungicidal effect of the combination was tested. The results showed that the combination of compound **D12** and FLC had a fungicidal effect at high concentrations (Figure 2D).

Compound D12 Exhibited Selective Inhibitory Effect on Fungal HDACs. Due to limited knowledge of fungal HDACs, there lacks well-established assays for the evaluations of fungal HDAC inhibitors. Using our previously developed fungal whole cell HDAC enzymatic assay,[16] the inhibitory activity of compound **D12** against fungal and human total HDACs was determined (Figure 3). As compared with TBA, compound **D12** generally showed improved inhibitory activity against fungal HDACs and decreased activity against human HDACs. Compound **D12** inhibited fungal HDACs stronger

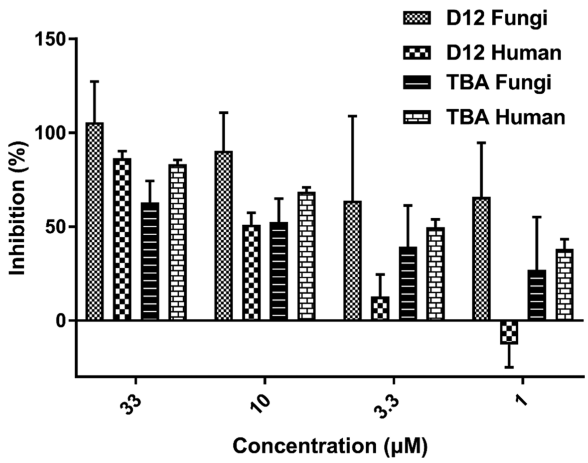

Figure 3. Inhibitory activity of compound **D12** and TBA against fungal (*C. albicans* 0304103) and human (HUVEC) total HDACs. Three independent experiments were performed.

https://dx.doi.org/10.1021/acs.jmedchem.0c01763
J. Med. Chem. 2021, 64, 1116−1126

than TBA at the same concentration. In contrast, compound **D12** was less active in inhibiting human HDACs than TBA. Moreover, compound **D12** also exhibited weaker inhibitory activity against human-derived HDAC1 (IC_{50} = 1034 nM) and HDAC6 (IC_{50} = 549 nM) than TBA and SAHA (Table 3). As

Table 3. Human HDAC1/6 Enzyme Inhibition (IC_{50}, nM)

compounds	HDAC1	HDAC6
D12	2226 ± 373.4	459 ± 56
TBA	752 ± 70.6	1.9 ± 0.6
SAHA	22.7 ± 0.9	28 ± 5

a result, the enhanced synergistic effect of compound **D12** might be associated with the increased selectivity of fungal HDACs over human HDACs. Furthermore, the cytotoxicity of compound **D12** alone and in combination with FLC on human normal cells was also tested. The result revealed that compound **D12** showed a relatively low toxicity to human umbilical vein endothelial cells (HUVEC, IC_{50} = 9.64 μM) and human normal liver cells (L02, IC_{50} = 11.46 μM, Table S4 in the Supporting Information). The combination of compound **D12** and FLC also revealed relatively low cytotoxicity (HUVEC, IC_{50} = 12.2 μM, Table S5 in the Supporting Information).

Combination of Compound D12 and FLC Reversed Azole Resistance in *C. albicans* by Regulating the Azole Target Gene (*ERG11*) and Efflux gene (*CDR1*). Previous research confirmed that azole resistance in *C. albicans* was correlated with the overexpression of *ERG11*, *CDR*, and *MDR1*.[20] *ERG11* is the target gene of azoles, and the efflux genes associated with azole resistance mainly include *CDR1*, *CDR2*, *MDR1*, and *FLU1*. To clarify the mechanism of the carboline derivative in reversing resistance, expression of several resistant genes treated with drugs alone or in combination was determined by the real-time reverse transcriptase polymerase chain reaction (RT-PCR). The overexpression (about 100-fold increase compared with the control) of *ERG11* could be detected after treated with FLC, which might be the main reason for the FLC resistance. Interestingly, the expression of *ERG11* was decreased to the basal levels after treated with the combination of FLC and compound **D12**. As for efflux pump genes, FLC upregulated the expression of *CDR1*, whereas the expression was downregulated to normal levels when FLC was used in combination with compound **D12**. FLC alone has no effect on the expression of *CDR2* and *MDR1*. On the contrary, compound **D12** alone upregulated the two genes. The upregulation of *CDR2* could be recovered to normal levels when compound **D12** was used in combination with FLC. However, the drug combination enhanced the *MDR1* levels by 8-fold. It is demonstrated that the combination of compound **D12** and FLC recovered azole sensibility in resistant *C. albicans* by regulating the azole target gene *ERG11* and efflux gene *CDR1* (Figure 4).

Combination of Compound D12 and FLC Blocks the Morphological Changes of *C. albicans*. Pathogenic *C. albicans* has various morphological states, termed fungal polymorphism,[21] including budded (yeasty) forms and hyphal forms.[22] The budded-to-hyphal transition process is crucial to fungi virulence[23] and the conversion exists during the whole process of *C. albicans* tissue invasion.[21] Photomicrographs of cells treated with different drugs are shown in Figure 5. Morphological conversion from yeast to hypha was still observed after the treatment with FLC or compound **D12** alone. In the group treated with FLC and compound **D12** in combination, only yeast fungi were observed. Thus, compound **D12** successfully assisted FLC to block the morphological transition of fungi and reduce the invasion ability of *C. albicans*.

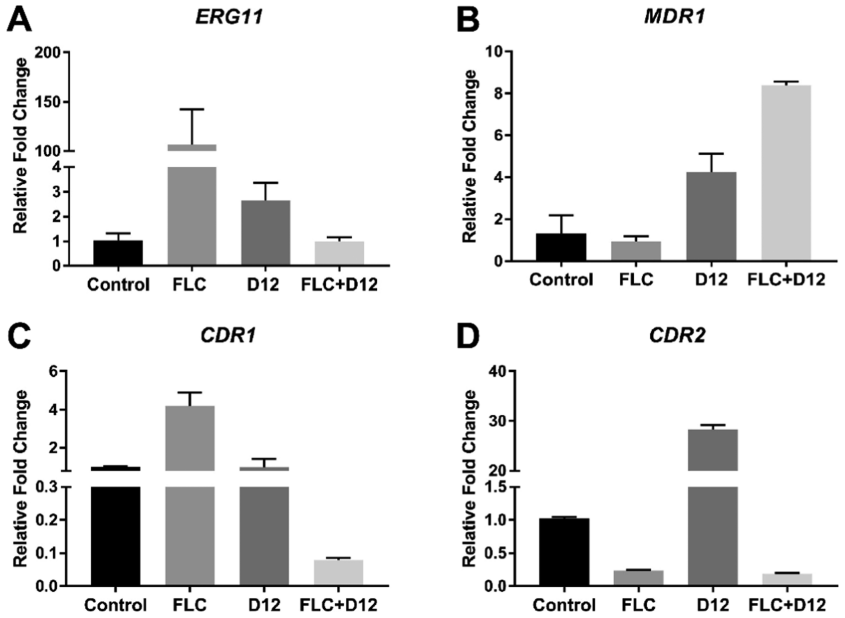

Figure 4. Expression of resistant genes of *C. albicans*. (A) Difference of *ERG11* expressed in each group. (B) Difference of *MDR1* expressed in each group. (C) Difference of *CDR1* expressed in each group. (D) Difference of *CDR2* expressed in each group. *C. albicans* (0304103) solution with initial concentrations of 1×10^6 cells/mL was divided into four groups, and, respectively, treated with DMSO (control), FLC (32 μg/mL), **D12** (32 μg/mL), and FLC + **D12** (32 + 32 μg/mL). RT-PCR was used to detect differences in the gene expression. Three independent experiments were performed.

https://dx.doi.org/10.1021/acs.jmedchem.0c01763
J. Med. Chem. 2021, 64, 1116−1126

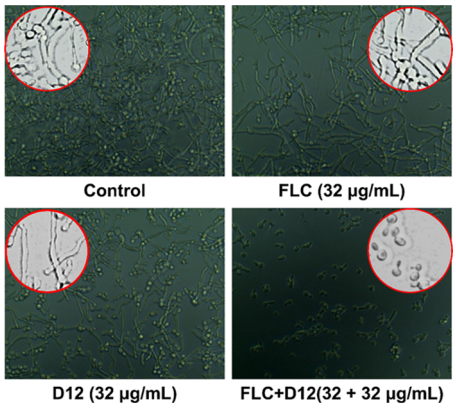

Figure 5. Hypha formation of *C. albicans* treated with **D12** and FLC alone or in combination. The initial concentration of *C. albicans* was 2 × 10^6 cells/mL. The Spider medium was used to induce the hyphae formation. The samples were observed and photographed after 3 h of incubation at 37 °C. Three independent experiments were performed.

Combination of Compound D12 and FLC Inhibits Fungal Biofilm Formation and Mature Biofilms. There is an intimate connection between fungal filamentation and biofilm formation because the hypha is an important part of mature fungal biofilm.[24] Biofilm formation is considered as a fungal survival mechanism related to drug resistance and immune escape.[25,26] The synergism of compound **D12** and FLC on *C. albicans* biofilm formation and disruption of preformed biofilms was investigated. The results showed that FLC or compound **D12** used alone could not inhibit fungal biofilm formation. Compound **D12** and FLC used in combination blocked the formation of fungal biofilms significantly at 64 μg/mL of compound **D12**, while the synergistic inhibition effect was not influenced by the concentrations of FLC (Figure 6A). The result is consistent with the time growth curves (Figure 2C). The disruption of preformed biofilms by the combination was also investigated (Figure 6B). Compound **D12** could cooperate with FLC to destroy mature biofilms only at a high concentration (64 μg/mL).

Compound D12 Enhanced the *In Vivo* Therapeutic Effect of FLC. The above results demonstrated the synergism of compound **D12** used in combination with FLC *in vitro*. Then, the *in vivo* antifungal potency of the drug combination was investigated. The mice models of candidiasis were established via tail vein injection of *C. albicans*. As shown in Figure 7A, compound **D12** was inactive, and FLC had a weak therapeutic effect ($P < 0.05$). In the group of drug combination, the antifungal potency was significantly enhanced ($P < 0.0001$). The combinational use of compound **D12** (10 mg/kg) and FLC (1 mg/kg) effectively reduced the kidney fungal burden in the infected mice. The fungal invasions in tissues were further monitored through the tissue section of the kidney to clearly understand the status of the fungal infection in mice and the effect of drug treatment. In the control group, a large number of fungal clusters stained deeply with amaranth (rod-shaped and spherical) were observed in the renal pelvis (arrow 1) but not obvious in the renal parenchyma cortex and medulla. When compound **D12** or FLC was used alone, there were also small clusters of fungal infiltration in the renal pelvis (arrow 2 and 3). In contrast, the fungal clusters were cleared in the renal pelvis or medulla in the group treated with compound **D12** and FLC in combination. The rod-shaped fungi (hyphal forms) observed in the drug-free group and single-drug group verified the morphological changes of budded-to-hyphal transition (200 fold) in mammals (Figure 7B). Thus, the combination of compound **D12** and FLC could reduce the colonization and dissemination of fungi in tissue and attenuate the virulence of fungi to the host by inhibiting the transition of *C. albicans* to the hyphal state.

CONCLUSIONS

In summary, novel carboline fungal HDAC inhibitors were designed, which provide a promising therapeutic strategy for combinational treatment of IFIs caused by azole-resistant *C. albicans*. In particular, compound **D12** had an excellent synergism with FLC against resistant *Candida* spp. The inhibition of hyphae and biofilm formation also demonstrated that the combination of compound **D12** and FLC could reduce fungal virulence. Compound **D12** reversed FLC resistance in *C. albicans* and enhanced efficacy of FLC probably because of downregulating the expression of the target gene *EGR11* and efflux gene *CDR1*. The *in vivo* antifungal potency was further validated in a mice candidiasis model, in which compound **D12** synergized with FLC to effectively clear the *C. albicans* burden in kidneys. Taken together, the fungal HDAC inhibitor **D12** represents a drug-like lead compound in the combinational treatment of candidiasis. Further research for fungal HDAC subtype selectivity, antifungal mechanisms, and lead optimization is proceeding.

EXPERIMENTAL SECTION

Chemistry. *General Methods.* ^{1}H NMR and ^{13}C NMR spectra were recorded on Bruker AVANCE600 spectrometers (Bruker Company, Germany), using tetramethylsilane (TMS) as an internal standard and $CDCl_3$ or DMSO-d_6 as solvents. Chemical shifts are given in ppm (δ). The mass spectra were recorded on an Esquire 3000 LC-MS mass spectrometer. Silica gel thin-layer chromatography was performed on precoated plates GF-254 (Qingdao Haiyang Chemical, China). All solvents and reagents were analytically pure, and no further purification was needed. All starting materials were commercially available. The purities of the compounds were determined by high-performance liquid chromatography (HPLC, Agilent 1260), and all final compounds exhibited purities greater than 95%.

*Methyl 2-(4-(3-Bromopropoxy)phenyl)acetate (**3**).* To a solution of methyl 2-(4-hydroxyphenyl)acetate (**2**, 5 g, 30.11 mmol) and K_2CO_3 (8.31 g, 60.22 mmol) in MeOH (150 mL) was added 1,3-dibromopropane (**1**, 9.12 g, 45.16 mmol) dropwise with stirring at room temperature. The reaction mixture was refluxed at 80 °C for 4 h. The solid was removed by filtration after the reaction mixture was cooled to room temperature. Then, the filtrate was concentrated under reduced pressure, H_2O (20 mL) was added, and the reaction mixture was extracted with EtOAc (40 mL × 3). The combined organic layer was washed with H_2O (30 × 3) and saturated NaCl (30 mL), dried over Na_2SO_4, filtered, and concentrated under reduced pressure. The residue was purified by column silica gel chromatography (hexane/EtOAc = 5/1) to give target compound **3** (5.5 g, 64.00%) as a colorless transparent liquid. ^{1}H NMR (600 MHz, DMSO-d_6): δ 7.17 (d, J = 8.6 Hz, 1H), 6.89 (d, J = 8.6 Hz, 1H), 4.06 (t, J = 6.0 Hz, 1H), 3.66 (t, J = 6.6 Hz, 1H), 3.61−3.57 (m, 2H), 2.23 (p, J = 6.3 Hz, 1H).

*tert-Butyl 8-Chloro-9-(3-(4-(2-methoxy-2-oxoethyl)phenoxy)-propyl)-1,3,4,9-tetrahydro-2H-pyrido[3,4-b]indole-2-carboxylate (**5l**).* To a solution of *tert*-butyl 8-chloro-1,3,4,9-tetrahydro-2*H*-pyrido[3,4-*b*]indole-2-carboxylate (**4l**, 0.24 g, 0.77 mmol) in dry DMF (3 mL), NaH (55 mg, 2.3 mmol) was added slowly at 0 °C.

https://dx.doi.org/10.1021/acs.jmedchem.0c01763
J. Med. Chem. 2021, 64, 1116−1126

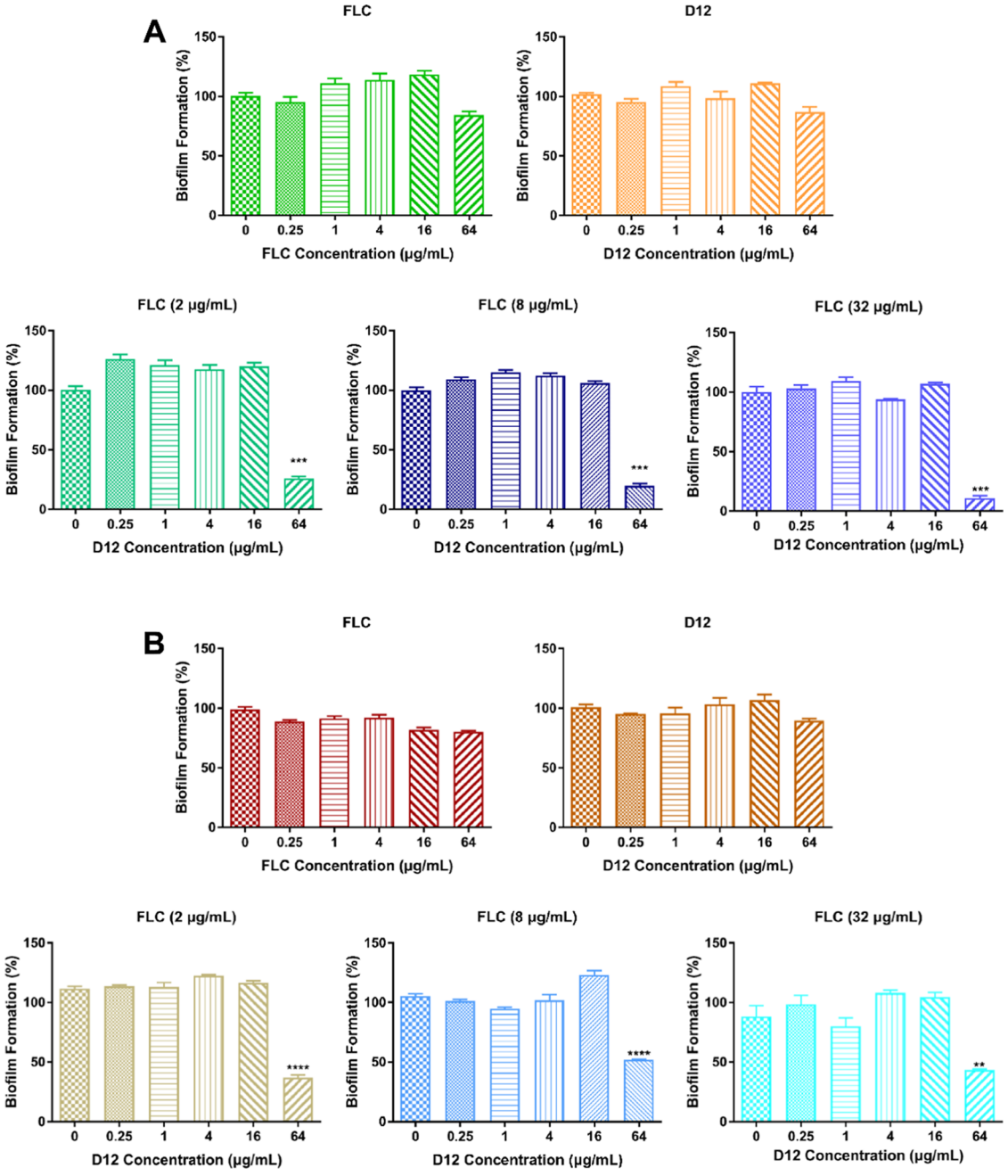

Figure 6. Inhibition of biofilm formation and disruption of mature biofilms treated with **D12** and FLC alone or in combination. (A) Inhibition of biofilm formation of *C. albicans* treated with **D12** and FLC alone or in combination. (B) Disruption of preformed biofilms of *C. albicans* treated with **D12** and FLC alone or in combination. The initial concentration of *C. albicans solution* was 2×10^6 cells/mL. The comparison between the two components was completed by the *t*-test. *** $P < 0.001$ compared to the control group. Three independent experiments were performed.

The reaction mixture was stirred at 0 °C for 5 min and then kept at room temperature for 30 min. Methyl 2-(4-(3-bromopropoxy)-phenyl) acetate (**3**, 0.33 g, 1.15 mmol) was added into the mixture and stirred at room temperature for 1 h. The reaction mixture was added dropwise into H_2O (10 mL) and extracted with EtOAc (20 mL × 3). The combined organic layer was washed with saturated NaCl (15 × 6), dried over Na_2SO_4, filtered, and concentrated under reduced pressure. The residue was purified by column silica gel chromatography (hexane/EtOAc = 15/1) to give target compound **5l** (0.31 g, 85.30%) as a transparent oil. ^{1}H NMR (600 MHz, $CDCl_3$): δ 7.34 (d, J = 7.5 Hz, 1H), 7.20−7.14 (m, 2H), 7.11 (d, J = 7.6 Hz, 1H), 6.98 (t, J = 7.7 Hz, 1H), 6.84−6.80 (m, 2H), 4.64 (s, 2H), 4.55−4.51 (m, 2H), 3.90 (t, J = 5.7 Hz, 2H), 3.68 (s, 3H), 3.67−3.63 (m, 2H), 3.57−3.53 (m, 2H), 2.73 (s, 2H), 2.28−2.22 (m, 2H), 1.49 (s, 9H).

*2-(4-(3-(8-Chloro-1,2,3,4-tetrahydro-9H-pyrido[3,4-b]indol-9-yl)-propoxy)phenyl)-N-hydroxyacetamide (**D12**).* To a solution of *tert*-butyl 8-chloro-9-(3-(4-(2-methoxy-2-oxoethyl)phenoxy)propyl)-1,3,4,9-tetrahydro-2*H*-pyrido[3,4-*b*]indole-2-carboxylate (**5l**, 0.30 g, 0.59 mmol) in dry dichloromethane (DCM, 7 mL), TFA (3.5 mL) was added dropwise with stirring at 0 °C. The reaction mixture was allowed to stir for 30 min to remove the protection of *tert*-butoxycarbonyl. Saturated $NaHCO_3$ was added dropwise into the mixture with stirring violently for 30 min after the addition of EtOAc (20 mL). The mixture was extracted with EtOAc (20 × 2) and the combined organic layer was washed with saturated NaCl, dried over

https://dx.doi.org/10.1021/acs.jmedchem.0c01763
J. Med. Chem. 2021, 64, 1116−1126

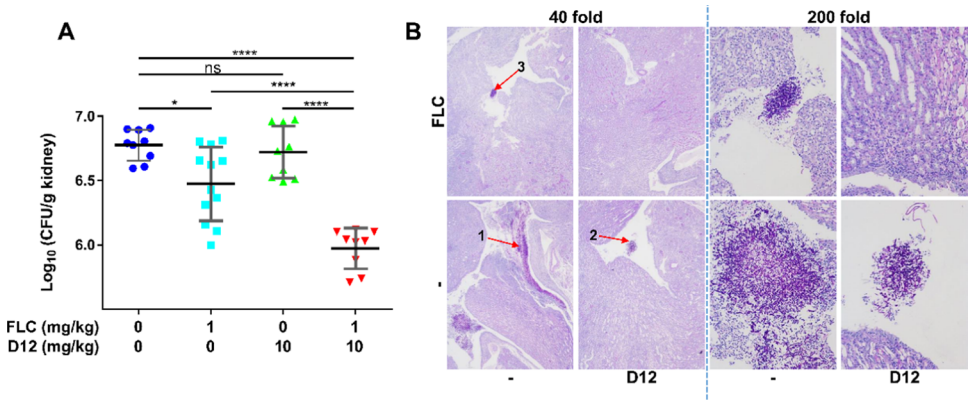

Figure 7. Combination of compound **D12** and FLC exhibits excellent therapeutic effects in mice candidiasis models. (A) Fungal burden in mice kidneys after treatment with different drugs. The infection model was established using 5×10^5 cells of *C. albicans* (0.04103) and the mice were divided into the control group, FLC group (1 mg/kg), **D12** group (10 mg/kg), and the combination group (FLC + **D12**, 1+10 mg/kg). The fungal burden of kidneys was determined after 5 days of treatment. The difference between the groups was compared by the *t*-test (* $p < 0.05$, ** $p < 0.01$, *** $p < 0.001$, **** $p < 0.0001$). (B) Kidney tissue sections after drug treatment in mouse models of candidiasis. (-) means treated with the vehicle, and the treatments were consistent with the kidney fungal burden experiment. The tissue was observed and photographed with a biological microscope under 40× and 200× fields of view, respectively.

Na_2SO_4, filtered, and concentrated under reduced pressure. The residue was used for the next reaction without further purification.

A solution of KOH (2.80 g, 200 mmol) in MeOH (7 mL) was added dropwise into a solution of $NH_2OH{\cdot}HCl$ (2.32 g, 33.5 mmol) in MeOH (12 mL) at 0 °C. Then, $MgSO_4$ (1 g, 8.31 mmol) was added into the reaction mixture and stirred at 0 °C for 30 min. The mixture was filtered to get a solution of NH_2OH. Methyl 2-(4-(3-(1,2,3,4-tetrahydro-9*H*-pyrido[3,4-*b*] indol-9-yl)propoxy)phenyl)-acetate obtained by the above reaction (0.27 g) was added into the solution of NH_2OH (17 mL, freshly prepared). The reaction was stirred at 45 °C for 2 h. The solvent was removed under reduced pressure. H_2O (3 mL) and 1N HCl were added into it to adjust the pH = 7−8. Then, the mixture was filtered and the residue was purified by HPLC to obtain target compound **D12** (0.12 g, 49%) as a white solid. ^{1}H NMR (600 MHz, DMSO-d_6): δ 10.57 (s, 1H), 7.35 (d, J = 7.4 Hz, 1H), 7.15 (d, J = 8.6 Hz, 2H), 7.07 (d, J = 7.4 Hz, 1H), 6.95 (t, J = 7.7 Hz, 1H), 6.82 (d, J = 8.6 Hz, 2H), 4.44 (t, J = 7.2 Hz, 2H), 3.92 (t, J = 5.9 Hz, 2H), 3.87 (s, 2H), 3.18 (s, 2H), 2.90 (t, J = 5.6 Hz, 2H), 2.56 (t, J = 5.4 Hz, 2H), 2.13−2.06 (m, 2H). ^{13}C NMR (151 MHz, DMSO-d_6) δ 167.8 (s), 157.5 (s), 137.8 (s), 131.1 (s), 130.8 (s), 130.4 (s), 128.6 (s), 122.7 (s), 120.1 (s), 117.1 (s), 115.5 (s), 114.7 (s), 108.8 (s), 64.9 (s), 43.4 (s), 42.0 (s), 41.6 (s), 39.0 (s), 32.0 (s), 22.4 (s). ESI-MS (m/z): 414.52 [M + 1]. ESI-HRMS: calcd for $C_{22}H_{24}ClN_3O_3$ m/z: $[M + H]^+$ = 414.1579; found $[M + H]^+$ = 414.1588, HPLC purity: 99.47%.

The synthesis of compounds **5a−m** and **D1−D11** was similar to the methods of **5l** and **D12**, respectively.

*2-(4-(3-(5-Chloro-1,2,3,4-tetrahydro-9H-pyrido[3,4-b]indol-9-yl)-propoxy)phenyl)-N-hydroxyacetamide (**D2**).* A light yellow solid, 0.091 g, yield 54%. ^{1}H NMR (600 MHz, DMSO-d_6) δ 10.58 (s, 1H), 7.35 (dd, J = 7.7, 0.9 Hz, 1H), 7.16 (d, J = 8.6 Hz, 2H), 6.99−6.93 (m, 2H), 6.87−6.82 (m, 2H), 4.18 (t, J = 6.9 Hz, 2H), 3.90−3.83 (m, 4H), 3.20 (s, 2H), 2.94−2.87 (m, 4H), 2.09−2.03 (m, 2H). ^{13}C NMR (151 MHz, DMSO) δ 167.8 (s), 157.4 (s), 137.3 (s), 136.9 (s), 130.4 (s), 128.65 (s), 124.7 (s), 124.3 (s), 121.4 (s), 119.3 (s), 114.7 (s), 108.8 (s), 107.3 (s), 64.8 (s), 43.7 (s), 42.0 (s), 38.9 (s), 29.6 (s), 24.4 (s). MS (ESI positive) m/z: 414.57 [M + 1]. ESI-HRMS: calcd for $C_{22}H_{24}ClN_3O_3$ m/z: $[M + H]^+$ = 414.1579; found $[M + H]^+$ = 414.1585.

*2-(4-(3-(6-Fluoro-1,2,3,4-tetrahydro-9H-pyrido[3,4-b]indol-9-yl)-propoxy)phenyl)-N-hydroxyacetamide (**D4**).* A light yellow solid, 0.096 g, yield 84%. ^{1}H NMR (600 MHz, DMSO-d_6) δ 10.61 (s, 1H), 7.41 (dd, J = 8.9, 4.4 Hz, 1H), 7.19 (dd, J = 9.8, 2.5 Hz, 1H), 7.16 (d, J = 8.6 Hz, 2H), 6.90 (td, J = 9.2, 2.5 Hz, 1H), 6.85 (d, J = 8.6 Hz, 2H), 4.20 (t, J = 6.9 Hz, 2H), 4.07 (s, 2H), 3.88 (t, J = 5.9 Hz, 2H), 3.20 (s, 2H), 3.10 (t, J = 5.7 Hz, 2H), 2.69 (t, J = 5.5 Hz, 2H), 2.12−2.02 (m, 2H). ^{13}C NMR (151 MHz, DMSO) δ 167.8 (s), 157.4 (s), 157.4 (d, J = 213.8 Hz), 135.0 (s), 133.0 (s), 130.8 (s), 130.4 (s), 128.7 (s), 127.2 (d, J = 9.9 Hz), 114.8 (s), 110.7 (d, J = 9.7 Hz), 109.0 (d, J = 25.8 Hz), 107.2 (d, J = 4.0 Hz), 103.1 (d, J = 23.2 Hz), 64.8 (s), 42.9 (s), 41.3 (s), 40.5 (s), 38.9 (s), 29.8 (s), 21.1 (s). ESI-HRMS: calcd for $C_{22}H_{24}FN_3O_4$ m/z: $[M + H]^+$ = 398.1874, $[M - H]^-$ = 396.1729; found $[M + H]^+$ = 398.1878 m/z, $[M - H]^-$ = 396.1751.

*2-(4-(3-(6-Bromo-1,2,3,4-tetrahydro-9H-pyrido[3,4-b]indol-9-yl)-propoxy)phenyl)-N-hydroxyacetamide (**D6**).* A light yellow solid, 0.18 g, yield 64%. ^{1}H NMR (600 MHz, DMSO-d_6) δ 10.60 (s, 1H), 7.57 (d, J = 1.9 Hz, 1H), 7.38 (d, J = 8.7 Hz, 1H), 7.18−7.13 (m, 3H), 6.84 (d, J = 8.6 Hz, 2H), 4.18 (t, J = 6.9 Hz, 2H), 3.96 (s, 2H), 3.87 (t, J = 5.9 Hz, 2H), 3.20 (s, 2H), 2.99 (t, J = 5.6 Hz, 2H), 2.62 (t, J = 5.3 Hz, 2H), 2.10−2.03 (m, 2H). ESI-HRMS: calcd for $C_{22}H_{24}BrN_3O_3$ m/z: $[M + H]^+$ = 460.1053, $[M - H]^-$ = 458.0908; found $[M + H]^+$ = 460.1063, $[M - H]^-$ = 458.0938.

*2-(4-(3-(7-Fluoro-1,2,3,4-tetrahydro-9H-pyrido[3,4-b]indol-9-yl)-propoxy)phenyl)-N-hydroxyacetamide (**D9**).* A light yellow solid, 0.24 g, yield 66%. ^{1}H NMR (600 MHz, DMSO-d_6) δ 10.63 (s, 1H), 7.40−7.36 (m, 1H), 7.27 (d, J = 8.9 Hz, 1H), 7.19−7.14 (m, 2H), 6.87−6.80 (m, 3H), 4.16 (t, J = 6.8 Hz, 2H), 3.97 (s, 2H), 3.88 (t, J = 5.8 Hz, 2H), 3.20 (s, 2H), 3.02 (t, J = 5.3 Hz, 2H), 2.69−2.61 (m, 2H), 2.09−2.03 (m, 2H). ^{13}C NMR (151 MHz, DMSO) δ 167.8 (s), 159.1 (d, J = 233.9 Hz), 157.4 (s), 136.3 (d, J = 12.2 Hz), 133.8 (s), 130.8 (s), 130.4 (s), 128.7 (s), 123.8 (s), 118.9 (d, J = 10.3 Hz), 114.7 (s), 107.2 (d, J = 29.9 Hz), 96.5 (d, J = 26.4 Hz), 64.8 (s), 42.9 (s), 41.3 (s), 40.5 (s), 38.9 (s), 29.6 (s), 21.2 (s). ESI-HRMS: calcd for $C_{22}H_{24}FN_3O_3$ m/z: $[M + H]^+$ = 398.1874, $[M - H]^-$ = 396.1729; found $[M + H]^+$ = 398.1888, $[M - H]^-$ = 396.1741.

*2-(4-(3-(7-Chloro-1,2,3,4-tetrahydro-9H-pyrido[3,4-b]indol-9-yl)-propoxy)phenyl)-N-hydroxyacetamide (**D10**).* A light yellow solid, 0.17 g, yield 78%. ^{1}H NMR (600 MHz, DMSO-d_6): δ 10.59 (s, 1H), 7.50 (d, J = 1.7 Hz, 1H), 7.38 (d, J = 8.3 Hz, 1H), 7.16 (d, J = 8.5 Hz, 2H), 6.97 (dd, J = 8.3, 1.8 Hz, 1H), 6.85 (d, J = 8.6 Hz, 2H), 4.17 (t, J = 6.9 Hz, 2H), 3.90−3.86 (m, 4H), 3.20 (s, 2H), 2.94 (t, J = 5.6 Hz, 2H), 2.59 (t, J = 5.4 Hz, 2H), 2.09−2.04 (m, 2H). ^{13}C NMR (151 MHz, DMSO) δ 167.7 (s), 157.4 (s), 136.58 (s), 136.4 (s), 130.4 (s), 128.7 (s), 126.1 (s), 125.7 (s), 119.1 (s), 114.8 (s), 109.6 (s), 107.9 (s), 64.9 (s), 43.4 (s), 41.9 (s), 38.9 (s), 29.7 (s), 22.3 (s). MS (ESI positive) m/z: 414.39 [M + 1]. ESI-HRMS: calcd for $C_{22}H_{24}ClN_3O_3$ m/z: $[M + H]^+$ = 414.1579 m/z; found $[M + H]^+$ = 414.1579.

Biology: Strains, Culture, and Agents. All of the strains used in this study are listed in Tables 1, 2, and S3 and derived from clinical isolates that were identified by standard mycological and molecular tests. The commonly used media are mainly as follows: the yeast

https://dx.doi.org/10.1021/acs.jmedchem.0c01763
J. Med. Chem. 2021, 64, 1116−1126

extract peptone dextrose (YEPD) liquid medium (1% yeast extract, 2% peptone, and 2% dextrose), RPMI 1640 medium (buffered with 0.165 M MOPS, 0.2% $NaHCO_3$, and 0.27% NaOH as the testing medium), and SDA medium (1% peptone, 4% glucose, and 2% agar). Strains were routinely resurrected in YEPD medium at 30 °C with continuous shaking. Compounds and FLC were diluted into 2 mg/mL solution using DMSO.

***In Vitro* Antifungal Activity Assay.** *In vitro* antifungal activity of the two compounds in synergy was measured by the checkerboard microdilution method in 96-well microtest plates. The assay was analyzed according to the methods described by the Clinical & Laboratory Standards Institute (CLSI, M27-A3) with a few modifications.[3] Briefly, exponentially grown *C. albicans* cells were harvested and resuspended in a fresh RPMI 1640 medium to a concentration of 10^3 cells/mL. The final concentrations for FLC and tested compounds ranged from 0.25 to 64 μg/mL and 2 to 64 μg/mL, respectively. Fungi were incubated at 35 °C for 48 h. The optical density at 630 nm (OD630) was determined using a microtiter plate reader while subtracting the background OD of each well. Synergy and antagonism were defined by FICIs of ≤0.5 and >4, respectively. An FICI > 0.5 but <4 was considered irrelevant.

Disk Diffusion Assay. About 1×10^4 cells were plated on the SDA medium or on SDA medium containing FLC (32 μg/mL) or **D12** (8 μg/mL), or both of them. Plates were incubated at 35 °C for 48 h and photographed to intuitively reflect the drug resistance of *C. albicans* (0304103) and the synergism of compound **D12** and FLC. Disk diffusion testing of drugs in combination was performed as follows. SDA plates (90 mm diameter) containing FLC (32 μg/mL) were used in this study. The surface of the medium was coated with approximately 10^5 *C. albicans* (0304103) cells by using a glass spreading rod. Disks containing different doses of compound **D12** (0, 2, 8, and 32 μg) were equidistantly placed onto the surface of the agar plate inoculated with fungi, and the plate was photographed 48 h after being incubated at 35 °C.

Growth Curve Assay. Growth curve assay was performed according to a previous method with a few modifications.[27] The exponentially grown *C. albicans* strain 0304103 was washed with PBS (phosphate buffer saline, 3 × 1 mL) and then resuspended in 5 mL of the RPMI 1640 medium to an initial concentration of 1.5×10^6 cells/mL and divided into different bottles. Samples added to different concentrations of compound **D12** and FLC were incubated in a shaking incubator (200 rpm) at 30 °C and counted at a specific time point (0, 6, 12, 24, and 48 h). Three independent experiments were performed.

Time Kill Curve Assay. The sample preparation was the same as that in the growth curve assay. The initial fungal concentration was 1.5×10^6 cells/mL and the samples treated with drugs alone or in combination were incubated in a shaking incubator (200 rpm) at 30 °C. Samples were taken at a specific time point (0, 6, 12, 24, 36, and 48 h), diluted and coated on the SDA medium, and cultured at 35 °C for 48 h. The fungal colonies in the medium were counted and the number of viable fungi was calculated. Three independent experiments were performed.

***In Vitro* Biofilm Formation Assay.** The experimental procedure was performed according to our previous methods with a few modifications.[28] Suspensions of *C. albicans* (0304103) cells (1.0×10^6 CFU/mL in the RPMI 1640 medium) were added into a 96-well microtest plate (100 μL per well) and incubated at 37 °C for 90 min for adhesion. The adherent cells were washed with PBS (3 × 100 μL) after the upper culture medium was removed. A fresh RPMI 1640 medium with or without drugs was then added to adherent cells. The final concentrations for FLC and tested compounds ranged from 2 to 32 μg/mL and 0.12 to 64 μg/mL, respectively. Then, the plates were incubated at 37 °C for another 24 h. A semiquantitative measure of biofilm formation was calculated by using the method of the XTT reduction assay. The optical density at 490 nm (OD490) was determined using a microtiter plate reader and three independent experiments were performed.

Disruption Assay of Preformed Biofilms. The experimental procedure was similar to the methods of the biofilm formation assay. Suspensions of *C. albicans* (0304103) cells (1.0×10^6 CFU/mL in the RPMI 1640 medium) were added into a 96-well microtest plate (100 μL per well) and incubated at 37 °C for 24 h to form a mature biofilm. The following operation was similar to the method of testing biofilm formation. Three independent experiments were performed.

***In Vitro* Hyphal Formation Assay.** The experimental procedure was performed according to reported methods with a few modifications.[29] Exponentially grown *C. albicans* cells resuspended in the Spider culture medium (10% Nutrient broth, 2% $NaHCO_3$, 2% $K_2HPO_4 \cdot 2H_2O$,) to 2×10^6 cells/mL were transferred to 12-well plates while each well was added with 1 mL of the suspension. Drugs used alone or in combination were added, and cells treated with DMSO were used as the control group. Cells were observed and photographed with an inversed fluorescence microscope after 3 h of incubation at 37 °C.

Inhibition of Human HDAC1/6. The assay was performed by quantitatively measuring the fluorescence intensity following an enzymatic reaction according to the reported method.[30] The dilution of compounds (5 μL) was added to a 40 μL of the reaction mixture (pH = 8.0) containing 25 mM Tris, 0.1 mM $MgCl_2$, 0.1 mg/mL BSA, 137 mM NaCl, 2.7 mM KCl, and HDAC6 (15 ng per well), so that the concentration of compounds ranged from 100 mM to 10 nM (3-fold dilution). The mixture was preincubated at room temperature for 5 min. Finally, the enzyme substrate (10 μM) was added, and the enzymatic reactions were conducted at 37 °C for 30 minutes in a final volume of 50 μL. The reactions were terminated by adding the termination solution (50 μL) for 30 min at room temperature. The IC_{50} values were calculated by measuring the fluorescence intensity at an excitation wavelength of 360 nm and an emission wavelength of 460 nm.

Inhibition of Fungal and Human Total HDACs. The fungal protoplast was extracted by the rapid yeast genomic DNA isolation kit (Sangon Biotech). About 100 mg of wet weight *C. albicans* cells exponentially grown were harvested and resuspended in 3 mL of snailase reaction buffer. Mercaptoethanol (2.4 μL) and snailase (50 μL, dissolved in snailase storage buffer to a concentration of 120 mg/mL) were added into the reaction buffer, and the sample was then incubated at 37 °C for 3 h. The lysate was centrifuged and the supernatant-removed protoplast was resuspended in 20 mL of PBS. The suspension and compounds were added into the 96-well microtest plates (100 μL for per well). The final concentration of tested compounds ranged from 1 to 100 μM. HDAC substrate Boc-Lys(Ac)-AMC was added into the plates at a concentration of 33 μM after the plates were incubated at 35 °C for 12 h. Then, the plates were incubated at 37 °C for another 6 h, and the reaction was terminated by adding 100 μL of the termination solution (2 mg/mL trypsin, 1% Nonidet P-40, 50 mM Tris-HCl (pH = 8), 137mM NaCl, 2.7 mM KCl, 1 mM $MgCl_2$) to each well and allowing the reaction to continue at 37 °C for 2 h. The reaction solution was transferred to a black 96-well plate, and the fluorescence intensity was measured at an excitation wavelength of 360 nm and an emission wavelength of 460 nm. The inhibition rate was calculated by the ratio of the fluorescence intensity of the compound group to that of the control group after subtracting the blank. Three independent experiments were performed. The human total HDAC Enzymatic assay was performed using HUVEC cells. Different from fungi, there was no need to prepare protoplasts, and about 15000 cells per well were seeded into 96-well transparent plates. After being incubated at 37 °C and 5% CO_2 atmosphere for 24 h, the compounds were added into the plates and the remaining operations were similar to the fungal HDAC enzymatic assay.

Quantification of the Gene Expression by Real-Time RT-PCR. Real-Time RT-PCR was performed according to the previous work with a few modifications.[31] Primers were synthesized by Sangon Biotech (Shanghai) Co., Ltd. and listed in Table S6 in the Supporting Information. *C. albicans* cells treated with different drugs alone or in combination were incubated in the YEPD medium at 35 °C for 24 h. For extraction of the total RNA of collected fungi, the Column Fungal RNAout kit (Tiandz, Inc.) was used according to the instructions. Reverse transcription was performed by using the PrimeScript RT

https://dx.doi.org/10.1021/acs.jmedchem.0c01763
J. Med. Chem. 2021, 64, 1116−1126

Master Mix kit (TaKaRa) through two steps (1. 37 °C for 15 min; 2. 85 °C for 5 s). The qRT−PCR was performed in the LightCycler Real-Time PCR system (Roche diagnostics, GmbH Mannheim, Germany), using SYBR Green I. Amplification of cDNA was carried out according to the established procedures: 95 °C for 30 s and then 40 cycles of 95 °C for 5 s, 60 °C for 34 s, 95 °C for 30 s, 60 °C for 60 s, and 95 °C for 15 s. Monitoring the fluorescence during cycling measures the threshold cycle. Fold changes in the gene expression was analyzed using the $2^{-\Delta\Delta Ct}$ method, with *ACT1* as the internal control.

Murine Model of Candidiasis. Female ICR (Institute of Cancer Research) mice (20−25 g each mouse) purchased from JOINN Laboratories (Certificate SCXK-2018-0006) were used in this experimentation. Four mice in each group and 5×10^5 cells *C. albicans* (0304103) were used to infect mice via lateral tail vein injection. Mice were then treated with the vehicle (1.5% glycerin and 0.5% Tween 80), 10 mg/kg compound **D12**, 1 mg/kg FLC, or the combination (**D12** + FLC) via intraperitoneal (IP) injections 24 h later. Treatments were administered continuously for 5 days after infection. The animal laboratory meets IACUC standards (Certificate SYXK-2017-0004). The kidneys were removed and homogenized. Diluent suspensions (1000-fold) were plated on the SDA medium containing chloramphenicol and incubated at 30 °C for at least 48 h to count the number of colonies and calculate the total fungal burden. The differences between groups were analyzed by analysis of variance (ANOVA).

Pathological Sections of Murine Kidneys. Two mice in each group and the infection and treatment of mice were consistent with the methods used in the murine model of candidiasis as mentioned above. Groups of mice were sacrificed 5 days after treatment with drugs alone or in combination. Fixed with 4% paraformaldehyde, sampled conventionally, dehydrated, embedded with paraffin, sliced (4 μm thick), and stained with hematoxylin−eosin (HE), the renal tissues removed from mice were observed (NIKON Eclipse Ci) and photographed (40× and 200×).

■ ASSOCIATED CONTENT

Supporting Information

The Supporting Information is available free of charge at https://pubs.acs.org/doi/10.1021/acs.jmedchem.0c01763.

Molecular formula strings of the target compounds (CSV);

synergism of TBA in combination with different first-line azole drugs; synergism of compounds **D1**−**12** in combination with azoles (VRC and ITC) against *C. albicans* (0304103); synergism of compound **D12** in combination with azoles (VRC and ITC) against various clinically isolated *C. albicans*, *C. krusei*, *C. auris*, *C. glabrata*, *C. tropicalis*, and *C. neoformans*; cytotoxicity of compound **D12** and SAHA alone or in combination with FLC; sequence of primers; the relative growth of various clinically isolated strains (Table 2) presented by the form of heat maps; protocols of the cytotoxicity assay; structural characterization; spectral data of target compounds; and HPLC spectra (PDF)

■ AUTHOR INFORMATION

Corresponding Authors

Na Liu − *Department of Medicinal Chemistry, School of Pharmacy, Second Military Medical University, Shanghai 200433, China;* orcid.org/0000-0002-3920-1008; Phone: +86 21 81871230; Email: 285939784@qq.com

Chunquan Sheng − *Department of Medicinal Chemistry, School of Pharmacy, Second Military Medical University, Shanghai 200433, China; School of Medicine, Tongji University, Shanghai 200072, China;* orcid.org/0000-0001-9489-804X; Phone: +86 21 81871201; Email: shengcq@smmu.edu.cn

Authors

Zhuang Li − *Department of Medicinal Chemistry, School of Pharmacy, Second Military Medical University, Shanghai 200433, China*

Jie Tu − *Department of Medicinal Chemistry, School of Pharmacy, Second Military Medical University, Shanghai 200433, China*

Guiyan Han − *Department of Medicinal Chemistry, School of Pharmacy, Second Military Medical University, Shanghai 200433, China*

Complete contact information is available at: https://pubs.acs.org/10.1021/acs.jmedchem.0c01763

Author Contributions

The manuscript was written through contributions of all authors. All authors have given approval to the final version of the manuscript.

Notes

The authors declare no competing financial interest.

■ ACKNOWLEDGMENTS

This work was supported by the National Natural Science Foundation of China (Grant 81973175 to N.L., Grant 81725020 to C.S.) and the Innovation Program of Shanghai Municipal Education Commission (Grant 2019-01-07-00-07-E00073 to C.S.).

■ ABBREVIATIONS LIST

HDAC, histone deacetylase; *C. albicans*, *Candida albicans*; IFIs, invasive fungal infections; ICU, intensive care unit; CYP51, lanosterol 14α-demethylase; JAK2, Janus kinase; FLC, fluconazole; TBA, tubastatin A; VRC, voriconazole; ITC, itraconazole; SARs, structure−activity relationships; DMF, dimethylformamide; TFA, trifluoroacetic acid; ZBG, zinc-binding group; FICI, fractional inhibitory concentration index; MIC_{80}, minimum concentration of 80% inhibition; *C. krusei*, *Candida krusei*; *Candida auris*, *C. auris*; *Candida glabrata*, *C. glabrata*; *Candida tropicalis*, *C. tropicalis*; *Cryptococcus neoformans*, *C. neoformans*; SDA, Sabouraud Dextrose Agar; YEPD, Yeast extract Peptone Dextrose; CLSI, Clinical & Laboratory Standards Institute; PBS, phosphate buffer saline; ICR, Institute of Cancer Research; OD, optical density; IP, intraperitoneal; HE, hematoxylin−eosin

■ REFERENCES

(1) Denning, D. W.; Bromley, M. J. Infectious Disease. How to bolster the antifungal pipeline. *Science* **2015**, *347*, 1414−1416.

(2) Gullo, A. Invasive fungal infections: the challenge continues. *Drugs* **2009**, *69*, 65−73.

(3) Li, D. D.; Zhao, L. X.; Mylonakis, E.; Hu, G. H.; Zou, Y.; Huang, T. K.; Yan, L.; Wang, Y.; Jiang, Y. Y. In vitro and in vivo activities of pterostilbene against *Candida albicans* biofilms. *Antimicrob. Agents Chemother.* **2014**, *58*, 2344−2355.

(4) Garnaud, C.; Champleboux, M.; Maubon, D.; Cornet, M.; Govin, J. Histone deacetylases and their inhibition in Candida species. *Front. Microbiol.* **2016**, *7*, 1238.

(5) Ostrosky-Zeichner, L.; Casadevall, A.; Galgiani, J. N.; Odds, F. C.; Rex, J. H. An insight into the antifungal pipeline: selected new molecules and beyond. *Nat. Rev. Drug Discovery* **2010**, *9*, 719.

(6) Nicola, A. M.; Albuquerque, P.; Paes, H. C.; Fernandes, L.; Costa, F. F.; Kioshima, E. S.; Abadio, A. K. R.; Bocca, A. L.; Felipe, M.

S. Antifungal drugs: new insights in research & development. *Pharmacol. Ther.* **2019**, *195*, 21−38.
(7) Xu, Y.; Wang, Y.; Yan, L.; Liang, R.-M.; Dai, B.-D.; Tang, R.-J.; Gao, P.-H.; Jiang, Y.-Y. Proteomic analysis reveals a synergistic mechanism of fluconazole and berberine against fluconazole-resistant *Candida albicans*: endogenous ROS augmentation. *J. Proteome Res.* **2009**, *8*, 5296−5304.
(8) Guo, F.; Yang, Y.; Kang, Y.; Zang, B.; Cui, W.; Qin, B.; Qin, Y.; Fang, Q.; Qin, T.; Jiang, D.; et al. Invasive candidiasis in intensive care units in China: a multicentre prospective observational study. *J. Antimicrob. Chemother.* **2013**, *68*, 1660−1668.
(9) Spitzer, M.; Robbins, N.; Wright, G. D. Combinatorial strategies for combating invasive fungal infections. *Virulence* **2017**, *8*, 169−185.
(10) Hill, J. A.; Cowen, L. E. Using combination therapy to thwart drug resistance. *Future Microbiol.* **2015**, *10*, 1719−1726.
(11) Shor, E.; Perlin, D. S. Coping with stress and the emergence of multidrug resistance in fungi. *PLoS Pathog.* **2015**, *11*, No. e1004668.
(12) Smith, W. L.; Edlind, T. D. Histone deacetylase inhibitors enhance *Candida albicans* sensitivity to azoles and related antifungals: correlation with reduction in CDR and ERG upregulation. *Antimicrob. Agents Chemother.* **2002**, *46*, 3532−3539.
(13) Mai, A.; Rotili, D.; Massa, S.; Brosch, G.; Simonetti, G.; Passariello, C.; Palamara, A. T. Discovery of uracil-based histone deacetylase inhibitors able to reduce acquired antifungal resistance and trailing growth in *Candida albicans*. *Bioorg. Med. Chem. Lett.* **2007**, *17*, 1221−1225.
(14) Li, X.; Cai, Q.; Mei, H.; Zhou, X.; Shen, Y.; Li, D.; Liu, W. The Rpd3/Hda1 family of histone deacetylases regulates azole resistance in *Candida albicans*. *J. Antimicrob. Chemother.* **2015**, *70*, 1993−2003.
(15) Pfaller, M.; Messer, S.; Georgopapadakou, N.; Martell, L.; Besterman, J.; Diekema, D. Activity of MGCD290, a Hos2 histone deacetylase inhibitor, in combination with azole antifungals against opportunistic fungal pathogens. *J. Clin. Microbiol.* **2009**, *47*, 3797−3804.
(16) Han, G.; Liu, N.; Li, C.; Tu, J.; Li, Z.; Sheng, C. Discovery of novel fungal lanosterol 14alpha-demethylase (CYP51)/histone deacetylase dual inhibitors to treat azole-resistant candidiasis. *J. Med. Chem.* **2020**, *63*, 5341−5359.
(17) Huang, Y.; Dong, G.; Li, H.; Liu, N.; Zhang, W.; Sheng, C. Discovery of janus kinase 2 (JAK2) and histone deacetylase (HDAC) dual inhibitors as a novel strategy for the combinational treatment of leukemia and invasive fungal infections. *J. Med. Chem.* **2018**, *61*, 6056−6074.
(18) Tu, J.; Li, Z.; Jiang, Y.; Ji, C.; Han, G.; Wang, Y.; Liu, N.; Sheng, C. Discovery of carboline derivatives as potent antifungal agents for the treatment of cryptococcal meningitis. *J. Med. Chem.* **2019**, *62*, 2376−2389.
(19) Gryder, B. E.; Sodji, Q. H.; Oyelere, A. K. Targeted cancer therapy: giving histone deacetylase inhibitors all they need to succeed. *Future Med. Chem.* **2012**, *4*, 505−524.
(20) White, T. C. Increased mRNA levels of ERG16, CDR, and MDR1 correlate with increases in azole resistance in *Candida albicans* isolates from a patient infected with human immunodeficiency virus. *Antimicrob. Agents Chemother.* **1997**, *41*, 1482−1487.
(21) Gow, N. A.; Van De Veerdonk, F. L.; Brown, A. J.; Netea, M. G. *Candida albicans* morphogenesis and host defence: discriminating invasion from colonization. *Nat. Rev. Microbiol.* **2012**, *10*, 112.
(22) Midkiff, J.; Borochoff-Porte, N.; White, D.; Johnson, D. I. Small molecule inhibitors of the *Candida albicans* budded-to-hyphal transition act through multiple signaling pathways. *PLoS One* **2011**, *6*, No. e25395.
(23) Grald, A.; Yargosz, P.; Case, S.; Shea, K.; Johnson, D. I. Small-molecule inhibitors of biofilm formation in laboratory and clinical isolates of *Candida albicans*. *J. Med. Microbiol.* **2012**, *61*, 109−114.
(24) Romo, J. A.; Pierce, C. G.; Chaturvedi, A. K.; Lazzell, A. L.; McHardy, S. F.; Saville, S. P.; Lopez-Ribot, J. L. Development of anti-virulence approaches for candidiasis via a novel series of small-molecule inhibitors of *Candida albicans* filamentation. *mBio* **2017**, *8*, e01991.
(25) Perlin, D. S.; Shor, E.; Zhao, Y. Update on antifungal drug resistance. *Curr. Clin. Microbiol. Rep.* **2015**, *2*, 84−95.
(26) Ramage, G.; Saville, S. P.; Thomas, D. P.; Lopez-Ribot, J. L. Candida biofilms: an update. *Eukaryotic Cell* **2005**, *4*, 633−638.
(27) Li, Z.; Liu, N.; Tu, J.; Ji, C.; Han, G.; Sheng, C. Discovery of simplified sampangine derivatives with potent antifungal activities against cryptococcal meningitis. *ACS Infect. Dis.* **2019**, *5*, 1376−1384.
(28) Li, Z.; Liu, N.; Tu, J.; Ji, C.; Han, G.; Wang, Y.; Sheng, C. Discovery of novel simplified isoxazole derivatives of sampangine as potent anti-cryptococcal agents. *Bioorg. Med. Chem.* **2019**, *27*, 832−840.
(29) Liu, N.; Zhong, H.; Tu, J.; Jiang, Z.; Jiang, Y.; Jiang, Y.; Jiang, Y.; Li, J.; Zhang, W.; Wang, Y.; Sheng, C. Discovery of simplified sampangine derivatives as novel fungal biofilm inhibitors. *Eur. J. Med. Chem.* **2018**, *143*, 1510−1523.
(30) Huang, Y.; Dong, G.; Li, H.; Liu, N.; Zhang, W.; Sheng, C. Discovery of janus kinase 2 (JAK2) and histone deacetylase (HDAC) dual inhibitors as a novel strategy for the combinational treatment of leukemia and invasive fungal infections. *J. Med. Chem.* **2018**, *61*, 6056−6074.
(31) Ji, C.; Liu, N.; Tu, J.; Li, Z.; Han, G.; Li, J.; Sheng, C. Drug repurposing of haloperidol: discovery of new benzocyclane derivatives as potent antifungal agents against Cryptococcosis and Candidiasis. *ACS Infect. Dis.* **2020**, *6*, 768−786.

https://dx.doi.org/10.1021/acs.jmedchem.0c01763
J. Med. Chem. 2021, 64, 1116−1126